Food Hydrocolloids 126 (2022) 107466

Contents lists available at ScienceDirect

Food Hydrocolloids

journal homepage: www.elsevier.com/locate/foodhyd

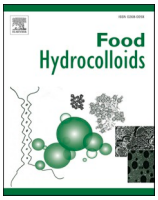

Ordered hydrocolloids networks as delivery vehicles of nutraceuticals: Optimal encapsulation of curcumin and resveratrol

Tianming Yao [a], Srinivas Janaswamy [b,*]

[a] Whistler Center for Carbohydrate Research, Department of Food Science, Purdue University, West Lafayette, IN, 47907, USA
[b] Dairy and Food Science Department, South Dakota State University, Brookings, SD, 57007, USA

ARTICLE INFO

Keywords:
Hydrocolloid network
Iota-carrageenan
Encapsulation
Delivery system
Polyphenols
Curcumin
Resveratrol

ABSTRACT

Nutraceutical compounds such as curcumin and resveratrol are effective for preventing and treating diabetes, cardiovascular disease, obesity and cancer. However, their unstable properties and water insolubility curtail the wholesome application as well as developing food supplements, functional foods and medicinal foods. Highly efficient and economical delivery systems are helpful to overcome this quandary. Among the several available carrier materials, hydrocolloids stand out tall due to their inbred non-toxic traits, cost-effectiveness and compatibility to humans. Herein, iota-carrageenan (IC), from the marine algae, has been chosen as the model hydrocolloid, which forms thermo-reversible gels and oriented fibers with ordered networks, and curcumin and resveratrol, as model nutraceuticals, have been encapsulated in the IC fibers for different time periods, namely for 1, 2, 3, 4 and 5 weeks to determine the optimal encapsulation time. The results demonstrate that encapsulation time dictates the overall entrapped amount in the IC network with an optimal duration of 3 weeks. The two nutraceuticals are readily protected from heat by the IC network and released in a sustained manner. The outcome offers an elegant opportunity to develop value-added delivery systems of nutraceuticals, in particular, and health promoting and disease preventing compounds, in general, based on the ordered hydrocolloid networks.

1. Introduction

The current dietary patterns comprising ultra-processed and high energy density foods coupled with sedentary lifestyles are deemed to impact human health toward setting up chronic diseases such as obesity, hypertension and diabetes (Canhada et al., 2020; Prentice & Jebb, 2003; Savoca & Miller, 2001). Toward this end, choice of healthy foods with nutraceutical function will be the foundation for good health. Among the several available dietary patterns in the human endeavor, vegetables and fruits are regarded as healthy choices due to their low calories, low sugar, high amounts of active vitamins and essential health promoting compounds, particularly polyphenols. Polyphenols possess several health promoting properties and indeed constitute as important natural micronutrients in the human diet (Gorzynik-Debicka et al., 2018). Their health benefits have been well established. For example, polyphenols presence in diet protects Type 2 Diabetes mellitus patients with low oxidative plasma status, improves cholesterol transportation efficiency and retards cardiovascular complications (Rasines-Perea & Teissedre, 2017; Castro-Barquero et al., 2020).

The bioactivity of polyphenols depends significantly on their chemical structure and molecular size. Small size molecules display higher bioavailability due to their direct absorption through epithelial cells of small intestine whilst larger ones get transported to the colon to be utilized by microbiota that modulate gut health (Aravind et al., 2021). The pH shift in the digestive tract regulates functional attributes as well (Bermúdez-Soto et al., 2007). In addition, high temperature exposure during food processing reduces the bioactivity (Patras et al., 2010). For example, anti-oxidation effect of polyphenols diminishes significantly during solar drying (Xing et al., 2017). Likewise, light affects the co-pigmentation of polyphenol complexes (Massounga Bora et al., 2018). These predicaments, indeed, restrain polyphenols bioavailability and their wholesome utility in food and non-food applications. Toward this end, delivery vehicles play a critical role not only to protect polyphenols from the external stresses but also to improve their bioavailability.

Cargoes such as porous starches, hydrocolloids, dextrin, liposomes, cyclodextrins, nanospheres, proteins and hydrocolloids are some of the successful examples (Fang & Bhandari, 2010). In this set,

* Corresponding author.
E-mail address: Srinivas.Janaswamy@sdstate.edu (S. Janaswamy).

https://doi.org/10.1016/j.foodhyd.2021.107466
Received 23 September 2021; Received in revised form 30 November 2021; Accepted 22 December 2021
Available online 27 December 2021

hydrocolloid-based carriers are cost-effective, environmentally friendly and highly efficient toward loading and releasing polyphenols. Hydrocolloids are water soluble polysaccharides that are used extensively in food, non-food, pharmaceutical and medical applications as thickeners, emulsifiers, viscosifiers and gelling agents. In this family, carrageenans gained special attention. These natural hydrocolloids extracted from edible seaweeds are used in food and dairy applications. Among the fifteen carrageenan types, known as of today, iota-carrageenan (IC) has been researched extensively due to its specific gelation properties influenced by the presence of salts that yield variable but manageable network structures (Elfaruk et al., 2021). It adopts a reversible transformation of ordered to disordered network structure and cation type (e.g. Na^+, K^+, and Ca^{2+}) modulates the molecular and packing structure (Janaswamy & Chandrasekaran, 2005). Among the studied cations, IC is flexible in the presence of sodium ions with its ability to form pseudo-polymorphic network structures (Janaswamy & Chandrasekaran, 2006).

We have embarked on a systematic study on the carrier systems of polyphenols based on the ordered hydrocolloid networks. Our research employed sodium iota-carrageenan (IC) as the model hydrocolloid to demonstrate the feasibility to encapsulate and release of curcumin (Janaswamy & Youngren, 2012), eugenol (Polowsky & Janaswamy, 2015) and a variety of drug molecules (Janaswamy et al., 2013). However, optimal encapsulation time for the maximum encapsulation efficiency has not yet been established. Herein, the objective is to evaluate the encapsulation quality of curcumin and resveratrol over different time intervals (from 1 to 5 weeks) in the sodium IC network. The thermal stability of encapsulated polyphenols has been identified and assessed. The release kinetics and associated structural changes have been established. The results reveal the optimum encapsulation time to be 3 weeks.

2. Materials and methods

2.1. Materials

Food grade iota-carrageenan (RE-PR-4018 and MW ~ 600 kDa) was gift from FMC Corporation, USA. Curcumin, resveratrol, sodium chloride and isopropanol were purchased from Sigma-Aldrich. Tokyo Chemical Industry Co., Ltd., Amresco LLC and Fisher Scientific, respectively. Distilled water from lab was used as needed.

2.2. Iota-carrageenan fibers

The IC solution was prepared based on our previous protocol (Polowsky & Janaswamy, 2015). Briefly, 100 mg of IC was dissolved into 10 mL of distilled water and heated in boiled water bath for 30 min with intermediate vortexing. Later, 60 mg of sodium chloride was added into the solution and continued heating until it is completely dissolved. The solution was cooled to room temperature and used to prepare oriented fibers. In a fiber puller (Fig. S1), a droplet of 20 mL was placed in between two glass rods (~0.5 mm distance) at 66% relative humidity (RH). Once the droplet was partially dried (around 2 h), the distance between the glass rods was slowly and carefully increased by turning the handles on the fiber puller until the fiber was stretched to about 2–3 mm in length. The fiber was then allowed to dry for 24 h and was cut from the glass rods and stored in a desiccator at 66% RH for further use.

2.3. Iota-carrageenan (IC):polyphenol complex preparation

The IC:polyphenol complexes preparation protocol is based on our established protocol (Janaswamy & Youngren, 2012). Briefly, as the chosen polyphenols curcumin and resveratrol are water insoluble, isopropanol was used to dissolve them. The polyphenol solution concentration of 0.1% was prepared by dissolving 20 mg of polyphenol in 19 mL isopropanol and later 1 mL of distilled water was added. The IC fibers were then soaked in the curcumin and resveratrol solutions for 7, 14, 21, 28 and 35 days, in separate containers, at the room temperature (20 °C). Subsequently, complex fibers were filtered and equilibrated at 66% RH for further analysis. The curcumin complexes are referred as CUR07, CUR14, CUR21, CUR28 and CUR35, and resveratrol complexes as RES07, RES14, RES21, RES28 and RES35, for brevity, during the rest of the discussion.

2.4. X-ray fiber analysis and unit cell dimensions

Synchrotron X-ray diffraction data on IC fibers and IC:polyphenol complexes were obtained using the 14-BMC beamline at BioCARS, Argonne National Laboratory (ANL), Chicago, IL, USA. The wavelength of the beam was 0.979 Å and the diffraction patterns were recorded on a CCD with 2 s exposure. The distance between fiber and detector was precisely estimated by dusting fibers with the calcite powder (3.035 Å characteristic spacing). The diffraction pattern center, detector to fiber distance, fiber tilt and rotation, Miller indices (h, k, l) for reflections and unit cell dimensions were estimated using FibreFix (Rajkumar et al., 2007) from CCP13 suite of programs. Reflection positions in each quadrant were measured and corresponding distance (ρ) between the origin and reflection point in the reciprocal space was estimated. The relationship between ρ, cylindrical radius (ξ) and vertical component (ζ) for a given reflection is given by: $\rho^2 = \xi^2 + \zeta^2$, where $\xi = a^*(h^2+hk+k^2)^{1/2}$ for a trigonal system ($a = b \neq c$, $\gamma = 120°$), $\xi = (a^{*2}h^2 + b^{*2}k^2)^{1/2}$ for an orthorhombic system ($a \neq b \neq c$, $\gamma = 90°$) and $\zeta = lc^*$. The dimensions of the reciprocal unit cell, a^*, b^* and c^*, as well as the Miller indices (h, k, l) for each reflection are estimated and the unit cell parameters a, b and c are calculated using in-house programs.

2.5. Melting behavior of IC and IC:polyphenol complexes

The Modulated Differential Scanning Calorimetry (mDSC) analysis on IC fibers, IC:polyphenol complexes and pure polyphenols was carried out using the DSC Q2000 from TA instruments (New Castle, DE). The equipment was calibrated with an Indium disk. About 1.0 ± 0.1 mg sample was packed in the Tzero aluminum hermetic pan and sealed tightly. The analysis was performed under 50 mL/min nitrogen flow. The temperature was ramped from 0 to 230 °C at a rate of 3 °C per minute with a modulation of ±0.68 °C for every 60 s. The tests were conducted in duplicate and average values are reported.

2.6. Polyphenol release from IC:polyphenol complexes and quantification

Concentration testing was performed at the room temperature (20 °C) using the Beckman Coulter DU 730 Life Science UV/Vis spectrophotometer. Isopropyl alcohol was used to solubilize curcumin and resveratrol. Initially, wavelength scan was performed in the range 200–600 nm to determine their optimum wavelength of absorbance. Subsequently, calibration curves were generated. Dissolution testing was performed, to generate a time release profile, by placing 1 mg of IC:polyphenol complex in 600 μL of distilled deionized water. The spectrometer was zeroed before the measurements with cuvette containing only water. Soon after adding the water, initial absorbance was read and later at every 2 min intervals for up to 2 h. The cuvette was shaken gently in between the measurements. The release amount of curcumin and resveratrol was calculated using their standard curves. Measurements from duplicate analysis are averaged and reported. The release kinetics are further analyzed by the DDSolver (Zhang et al., 2010).

2.7. Statistical analysis

Experimental data from technical replications were presented as mean ± standard error. All statistical differences in this study were calculated by analysis of variance (ANOVA). Fisher's least significant difference (LSD) tests and Bonferroni adjustment ($p < 0.05$) was adopted to evaluate group differences.

3. Results and discussion

3.1. Structural characterization

In order to understand the influence of encapsulation time on the loaded amount in the hydrocolloid matrix, curcumin and resveratrol have been encapsulated in the iota-carrageenan (IC) fibers for 7, 14, 21, 28 and 35 days. The corresponding X-ray fiber diffraction patterns are shown in Fig. 1. The uniformly sharp and small-sized Bragg reflections extending up to 2.7 Å in all the diffraction patterns indicate clearly the long-range lateral ordering of IC helices in the fibers that are uniaxially oriented and polycrystalline. In the case of IC, the first reflection on the meridian (an imaginary vertical line passing through the center of the diffraction pattern) is noticed on the 3rd layer line portraying the three-fold helical structure of IC. These Bragg reflections could be indexed on a trigonal cell of $a = 24.2$ and $c = 13.1$ Å that agree well with the reported values (Janaswamy & Chandrasekaran, 2001).

In the case of IC:curcumin and IC:resveratrol complexes the meridian is also on the 3rd layer line suggesting the intact three-fold helical structure of IC even in the presence of polyphenols. However, the number of Bragg reflections and their size and intensity differences along with changes in their positions after incorporating curcumin and resveratrol in the IC network indicate structural differences among the complexes. More significantly, differences between the IC:curcumin and IC:resveratrol complexes are quite evident from the basal net distribution. In the case of IC:curcumin, the complex with 7 days encapsulation yields unit cell dimensions of $a = 59.2(1)$, $b = 13.7(1)$ and $c = 13.2(1)$ Å. On the other hand, IC:resveratrol adapts a hexagonal net of $a = 56.2(1)$, $c = 13.1(1)$ Å. The basal net area of IC, IC:curcumin and IC:resveratrol is 507.2, 811.0 and 2735.2 Å^2, respectively. These variations in the unit cell dimensions suggest undoubtedly differences in the affinity of curcumin and resveratrol to the IC helices and their ability to pack in the IC network. The hydroxyl groups of curcumin and resveratrol appear to offer the required polarity (Feng & Liu, 2009) toward promoting hydrogen bonding interactions within the IC network. Interestingly, resveratrol is small in size compared to curcumin, and thus it might experience less spatial hindrance with the water pockets in the IC network leading to complexation. Overall, variations in the affinity of curcumin and resveratrol molecules with the IC helices along with changes in their molecular sizes in altering the inter helical interactions among the IC helices seem to be the root cause for the observed variations in the unit cell dimensions and in-turn the packing arrangements.

The unit cell dimensions from all the complexes are listed in Table 1. Overall, there are subtle changes in the values as a function of the encapsulation time. This is reasonable as the micro-structure of IC in fibers could not be altered once the preparation process is fixed and the loading amount of polyphenol is more dependent on the available water pockets in the IC network than the encapsulation time. This observation is in agreement with the thermal analysis (section 3.2), which indicates that prolonged encapsulation does not influence the internal structure of the IC complexes. However, the time of encapsulation has significant impact on the total encapsulated amount as well as the release process (section 3.3).

Table 1
Unit cell dimensions of iota-carrageenan (IC) (hexagonal lattice: $a = b \neq c$, $\alpha = \beta = 90°$, $\gamma = 120°$), IC:curcumin complexes (orthorhombic lattice: $a \neq b \neq c$, $\alpha = \beta = \gamma = 90°$) and IC:resveratrol complexes (hexagonal lattice).

Sample	a (Å)	b (Å)	c (Å)	α (°)	β (°)	γ (°)
IC	24.0	24.0	13.1	90	90	120
CUR07	59.2	13.7	13.2	90	90	90
CUR14	59.0	13.7	13.1	90	90	90
CUR21	59.5	13.6	13.1	90	90	90
CUR28	59.7	13.7	13.2	90	90	90
CUR35	59.0	13.7	13.1	90	90	90
RES07	56.2	56.2	13.1	90	90	120
RES14	56.5	56.5	13.1	90	90	120
RES21	56.8	56.8	13.1	90	90	120
RES28	56.1	56.1	13.0	90	90	120
RES35	56.0	56.0	13.1	90	90	120

3.2. Thermal stability

The IC:curcumin and IC:resveratrol samples along with pure curcumin, resveratrol and IC fibers were subjected to thermal analysis to understand the role of heat on the encapsulated curcumin and resveratrol. The thermal profiles are depicted in Fig. 2 and the melting and crystallization peak temperatures are compared in Table 2.

The IC fibers display crystallization and melting peaks at around 178 and 192 °C, respectively, portraying their semi-crystalline nature. During heating, IC chains in the amorphous regions re-associate and release energy resulting in the observed exothermic peak. On the other hand, in the crystalline regions, known as junction zones, IC chains absorb heat and melt leading to an endothermic peak. During the fiber preparation, semi-solid solution of IC was stretched so that IC chains could orient along the fiber axis leading to order network composed of water pockets. Thus, IC solution concentration, cation type and relative humidity at which fibers are being stretched influence the IC network formation, and these changes would readily reflect thermal profiles and more

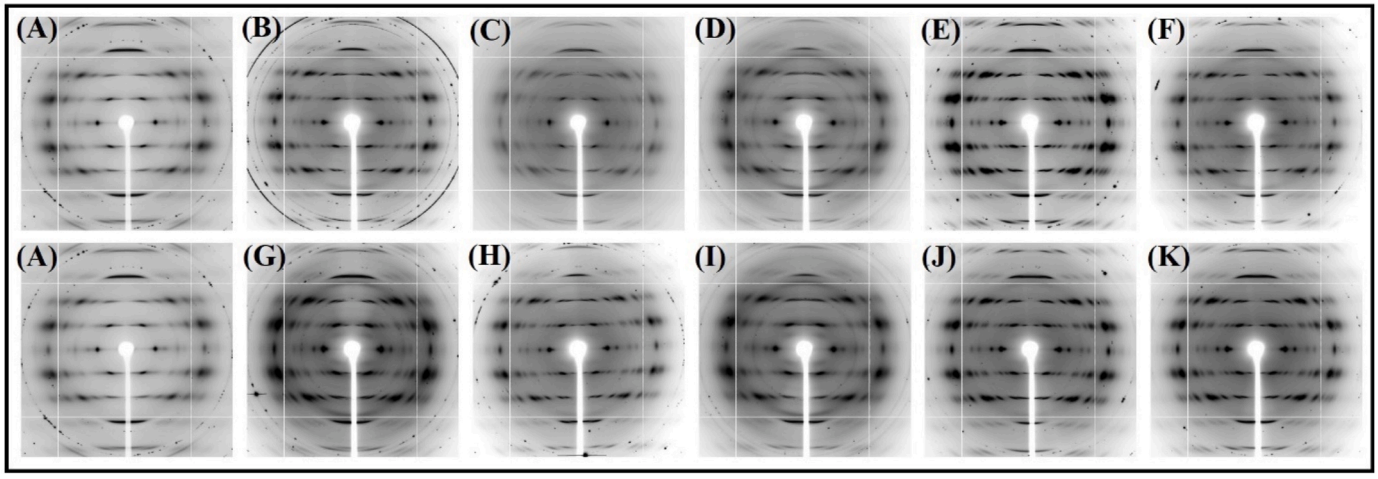

Fig. 1. X-ray fiber diffraction patterns of iota-carrageenan (IC) and its complexes with curcumin and resveratrol. (A) Pure IC, and IC:curcumin and IC:resveratrol complexes with 7, 14, 21, 28 and 35 days encapsulation are at (B), (C), (D), (E) and (F), (G), (H), (I), (J) and (K), respectively.

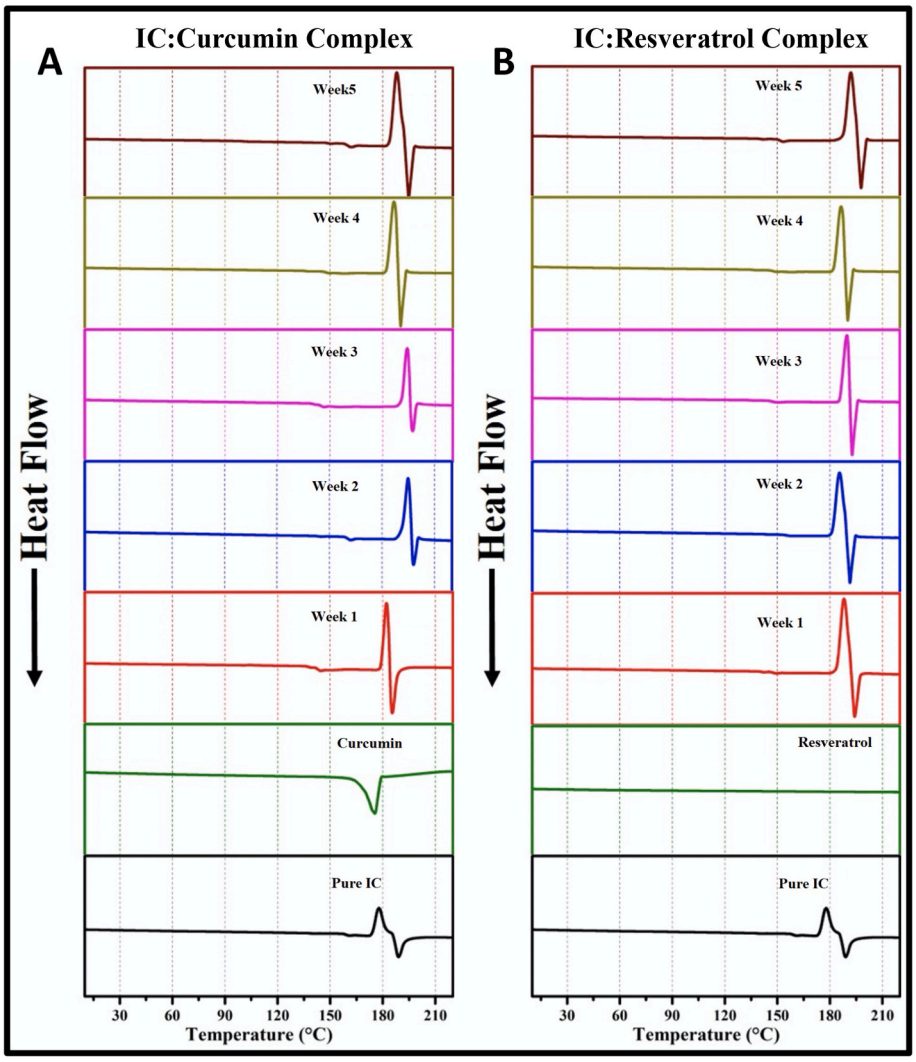

Fig. 2. The mDSC profiles of (A) IC:curcumin and (B) IC:resveratrol complexes that demonstrate the heat protection of curcumin and resveratrol by the IC fibers upon encapsulation (exothermic: up and endothermic: down). The complexes of different encapsulation times from 1 to 5 weeks are presented along with pure IC fiber and curcumin and resveratrol powders. The resveratrol melting peak at 261 °C is not shown.

Table 2
The crystalline and melting peaks of iota-carrageenan (IC), curcumin, resveratrol, IC:curcumin and IC:resveratrol complexes[A,B].

Sample	Crystallization		Melting	
	Temperature (°C)	Enthalpy (J/g)	Temperature (°C)	Enthalpy (J/g)
IC	178.51 ± 0.97	120.3	191.98 ± 4.14	72.17
Curcumin			175.48 ± 0.08	149.8
CUR07	182.22 ± 0.55^{c}	140.0	185.38 ± 2.52^{b}	96.49
CUR14	190.22 ± 2.53^{b}	170.7	196.70 ± 0.54^{a}	42.32
CUR21	194.06 ± 1.33^{a}	155.1	196.79 ± 1.04^{a}	51.29
CUR28	192.98 ± 2.18^{ab}	175.3	196.54 ± 2.18^{a}	20.56
CUR35	190.44 ± 0.70^{b}	303.2	196.23 ± 2.12^{a}	117.6
Resveratrol			261.24 ± 0.39	254.0
RES07	187.12 ± 1.48^{bc}	161.0	191.66 ± 3.41^{b}	164.5
RES14	184.20 ± 1.95^{d}	171.0	190.58 ± 1.20^{b}	168.1
RES21	189.44 ± 0.46^{b}	237.8	194.48 ± 2.58^{ab}	186.6
RES28	185.04 ± 1.80^{cd}	219.2	191.09 ± 1.36^{b}	125.8
RES35	192.67 ± 1.06^{a}	270.2	197.44 ± 0.43^{a}	128.2

[A]The data are presented as the mean of triplicate measurements.
[B]The values in each column with different superscripts are significantly different ($p < 0.05$).

significantly in terms of the melting and crystallization temperature.

The pure curcumin and resveratrol melt at 175 and 261 °C, respectively, indicating their crystalline nature. The thermal profiles of IC:curcumin and IC:resveratrol complexes are different from those of IC and pure polyphenols. In the complexes, both the crystalline and melting peaks are sharper and occur at higher temperature than the original IC fibers. Interestingly, melting peaks of curcumin and resveratrol are not seen in the complexes suggesting their heat protection by the IC fibers. In the case of curcumin, the exothermic peak of three-week complex occurs at 194 °C, which is 16 °C higher than the pure IC fibers. Similar higher crystalline temperature, 14 °C higher than the IC fibers, is noticed in the IC:resveratrol complexes. Furthermore, IC:polyphenol complexes display a higher crystallization enthalpy than the pure IC fibers, implying that there might be a chance for guest molecules to form stable crystalline network within the IC network and with higher thermal stability. The encapsulation time seems to have little-to-none influence on the thermal profiles despite subtle changes in the peak positions for both polyphenols. The melting temperature of IC:curcumin complexes is roughly 5 °C higher than the original fibers. The crystalline peaks appear at 182, 190, 194, 193 and 190 °C for 1, 2, 3, 4 and 5 week encapsulation, respectively. Similar phenomenon is noticed with the IC:resveratrol complexes as well. The melting peak is roughly 4 °C higher than the IC fibers, and crystalline peaks emerge at 187, 184, 189,185 and 192 °C,

respectively.

3.3. Release kinetics of curcumin and resveratrol from the complexes

The flexibility of IC chains in the presence of monovalent sodium ions has been reported to host a variety of guest molecules with variable size due to tunable inter-helical space in the network (Janaswamy et al., 2013). In this regard, the sodium IC employed in this research could readily hold curcumin and resveratrol molecules. The release profiles of curcumin and resveratrol from the IC fiber network at different encapsulation times are shown in Fig. 3.

The curcumin releases in a continuous manner (Fig. 3A). It reaches saturation at 48, 48, 46, 42 and 40 min from the 1, 2, 3, 4 and 5 week complexes, respectively. The corresponding release amount is 0.179, 0.227, 0.284, 0.306 and 0.307 μg/mg, in the same order, suggesting that the 4 week encapsulation could be the optimal time for encasing curcumin in the IC network. On the other hand, resveratrol release occurs in a two stage manner (Fig. 3B). The first stage starts from 0 min to 30, 30, 36, 38, 40 min for the 1, 2, 3, 4 and 5 week complexes, respectively, and the second stage saturates at 54, 60, 50, 56 and 58 min, in the same order. The two-stage release nature means more complicated interactions between the resveratrol molecules and IC chains are taking place during encapsulation. The final loading amount of resveratrol is 0.331, 0.469, 0.662, 0.659 and 0.685 μg/mg for the 1, 2, 3, 4 and 5 week complexes, respectively, directing 3 weeks as the optimal encapsulation time.

Overall, prominent differences among the curcumin and resveratrol encapsulation including release amount, release kinetics, encapsulation time and mechanisms of complexing are noticed. The maximum release amount of curcumin and resveratrol is found to be 0.307 and 0.685 μg/mL, respectively, both occurring at 5 weeks of encapsulation. Curcumin is a larger molecule with a molar mass of 368.39 g/mol, while the resveratrol is relatively a small molecule with molecular weight of 228.25 g/mol. Their differences in the molecule size and weight appears to be responsible for the observed variations.

The release kinetics have been analyzed through a series of mathematic models and results are summarized in Table 3. The superior fitness was concluded by comparing the R square (R^2) and Akaike Information Criteria (AIC) values. The AIC is a measure of the best fit based on the maximum probability with a smallest value. A set of 14 models, namely zero order, first order, Higuchi, Korsmeyer-Peppas, Hixson-Crowell, Hopfenberg, Baker-Londsale, Makoid-Banakar, Peppas-Sahlin, Quadratic, Weibull, Logistic, Gompertz and probit have been selected based on the published literature (Costa & Lobo, 2001; Gao, 2011). The curcumin complexes are found to be most compatible with the Korsmeyer-Peppas model with the R^2 and AIC of 0.9856 and −105.48, respectively. In contrast, the two release stages of resveratrol are best fitted with the Makoid-Banakar and Korsmeyer-Peppas models, respectively (Fig. S2). The Korsmeyer-Peppas model is a semi-empirical model based on the Fickian diffusion law to explain hydrophobic molecules diffusion from hydrophilic matrices (Korsmeyer et al., 1983) such as polymer blends, mesoporous materials and tablets (Avachat & Kotwal, 2007; Heikkilä et al., 2007; Ngwuluka et al., 2016; Sriamornsak et al., 2007). In the case of IC complexes employed in this study, IC network is highly hydrophilic and both curcumin and resveratrol are hydrophobic molecules; indeed, it is a suitable scenario to apply the Korsmeyer-Peppas model to interpret the releasing kinetics. In this model, the parameter K is a kinetic constant that is proportional to the release speed, while n refers to different types of releasing mechanisms. It follows the Fickian law when $n = 0.5$, non-Fickian transportation for $0.5 < n < 1.0$, case 2 transport when $n = 1$ and super case 2 transport when $n > 1$ (Korsmeyer & Peppas, 1981). The modeling parameters for both the complexes are listed in Tables 4–6. In case of IC:curcumin complexes, the parameter K increases along with encapsulation time from 1 to 4 weeks. The increasing releasing speed might be caused by the elevation of total encapsulation amount. The parameter n is larger than one, suggesting the super case 2 transportation, meaning that curcumin release follows the diffusion mechanism along with simultaneous collapse of the IC network (Korsmeyer et al., 1983). In the case of IC: resveratrol, release kinetics are more complicated than the IC:curcumin and contains two different release mechanisms (Fig. 3B). During the first stage, Makoid-Banakar model yields best fit with R^2 of 0.9916 and AIC = −126.66, however, first-order model also has an equally high R^2 of 0.9901 and AIC of −121.46. The Makoid-Banakar model is an empirical model without mathematical treatment and thus it could neither provide essential information about the encapsulate diffusion rate nor details about the kinetic properties (Costa & Sousa Lobo, 2003). In this regard, the first-order model is chosen as the appropriate model to understand the release mechanism. First-order model is more about solid particle diffusion in a liquid media from porous surfaces. The release rate of substance is proportional to concentrations of liquid and solid parts (Gibaldi & Feldman, 1967). The proportionality constant K increases along with the release rate. During the first stage, K is larger for 1 and 2 weeks encapsulation but smaller during the later periods. This can be explained by impaired resveratrol loading during the first two weeks of encapsulation. Moreover, it can be influenced by solid surface area that

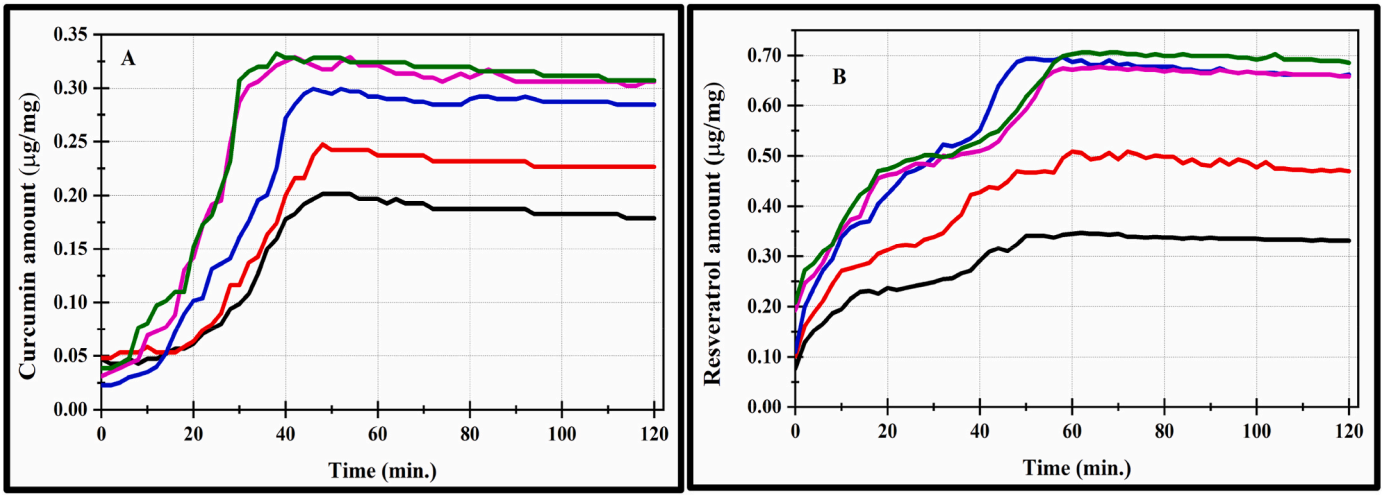

Fig. 3. The release profiles of curcumin and resveratrol from the (A) IC:curcumin and (B) IC:resveratrol complexes, respectively. The black, red, blue, pink, and green lines correspond to 7, 14, 21, 28 and 35 days of encapsulation, respectively. (For interpretation of the references to colour in this figure legend, the reader is referred to the Web version of this article.)

Table 3
The R^2 and AIC comparison of different models for the curcumin and resveratrol release from the iota-carrageenan fiber network.

Model	Equation	Curcumin		Resveratrol			
				Stage 1		Stage 2	
		R^2	AIC	R^2	AIC	R^2	AIC
Zero-order	$F=F_0+k_0*t$	0.9427	−81.18	0.8740	−73.78	0.9376	−70.25
First-order	$F=Fmax*\{1-exp[-k_1*(t-Tlag)]\}$	0.9369	−81.34	0.9901	−121.42	0.9367	−68.08
Higuchi	$F=F_0+k_H*t\hat{}0.5$	0.7866	−56.19	0.9603	−98.03	0.7637	−52.95
Korsmeyer-Peppas	$F=F0+k_{KP}*t\hat{}n$	0.9856	−105.48	0.9603	−96.04	0.9960	−86.37
Hixson-Crowell	$F = 100*[1-(1-k_{HC}*t)\hat{}3]$	0.9369	−81.36	0.8742	−73.81	0.9375	−70.23
Hopfenberg	$F = 100*[1-(1-k_{HB}*t)\hat{}n]$	0.9734	−95.78	0.8742	−71.81	0.9376	−68.25
Baker-Lonsdale	$3/2*[1-(1-F/100)\hat{}(2/3)]-F/100 = k_{BL}*t$	0.6516	−48.89	0.9388	−88.96	0.9165	−66.46
Makoid-Banakar	$F = k_{MB}*(t-Tlag)\hat{}n*Exp[-k*(t-Tlag)]$	0.9757	−95.50	0.9916	−126.66	0.6451	−10.15
Peppas-Sahlin	$F = k_1*t\hat{}m + k_2*t\hat{}(2*m)$	0.9763	−95.97	0.9815	−112.08	0.9355	−65.83
Quadratic	$F = 100*(k_1*t\hat{}2+k_2*t)$	0.9761	−97.79	0.9892	−121.35	0.9470	−70.39
Weibull	$F = 100*\{1-Exp[-(t\hat{}\beta)/\alpha]\}$	0.9739	−96.13	0.9706	−102.33	0.9021	−60.41
Logistic	$F = 100*Exp[\alpha+\beta*log(t)]/\{1+Exp[\alpha+\beta*log(t)]\}$	0.9739	−96.12	0.7843	−62.49	0.9550	−72.50
Gompertz	$F = 100*Exp\{-\alpha*Exp[-\beta*log(t)]\}$	0.9690	−92.85	0.7854	−62.59	0.9517	−71.57
Probit	$F = 100*\Phi[\alpha+\beta*log(t)]$	0.9714	−94.41	0.7850	−62.55	0.5853	−11.64

Table 4
The Korsmeyer-Peppas model parameters for IC:Curcumin.

Samples	R^2	Parameters		
		K	n	F_0
CUR07	0.9953	2.312E-06	2.974	0.045
CUR14	0.9886	3.735E-06	2.877	0.049
CUR21	0.9886	4.646E-04	1.686	0.019
CUR28	0.9856	7.225E-04	1.700	0.027
CUR35	0.9794	1.878E-04	2.096	0.046

Table 5
The first-order model parameters for IC:Resveratrol during stage one release.

Samples	R^2	Parameters		
		K	Tlag	Fmax
RES07	0.9865	0.120	−3.333	0.252
RES14	0.9917	0.105	−3.595	0.342
RES21	0.9901	0.049	−5.389	0.607
RES28	0.9881	0.066	−6.478	0.540
RES35	0.9854	0.069	−6.898	0.547

Table 6
The Korsmeyer-Peppas model parameters for IC:Resveratrol during stage two release.

Samples	R^2	Parameters		
		K	n	F_0
RES07	0.9507	0.009	0.744	0.240
RES14	0.9522	0.021	0.613	0.330
RES21	0.9648	0.015	0.985	0.428
RES28	0.9960	2.345E-05	2.772	0.498
RES35	0.9971	3.249E-04	1.951	0.499

cannot be accurately controlled during the experimental protocol adopted in this research. The first-order kinetics are usually applied on the release of molecules without destruction of delivery vehicles, suggesting that there are stronger interactions between resveratrol and IC matrix, which maintains the complex network structure, while only the resveratrol molecules from the outer surface of IC fibers diffuse out during the first release stage. Then, during the second stage, with continuous resveratrol diffusion, the hydrophilic IC network collapses easily in water and results in different release kinetics. Thus, the Korsmeyer-Peppas model stands out to be the most appropriate to understand the stage two release kinetics with the R^2 of 0.9960 and AIC of −86.37. The parameter 'n' value increases along with the encapsulation time, indicating different releasing speed and kinetics among the five weeks of encapsulation. The n value is larger than 0.5 but smaller than 1 for the first three weeks and larger than 1 for 4 and 5 weeks, indicating an anomalous diffusion mechanism. This mechanism that includes the non-Fickian and super case 2 transportation in a sequential order (for stage 1 and 2 release, respectively) describes the unique encapsulation and releasing traits for IC:resveratrol. The release kinetics could as well be influenced by water absorption and swelling by the IC matrix, as in stage two, and the release could be caused by the relaxation of the carrageenan network structure.

Overall, the outlined two different mechanisms could help to comprehend the molecular interactions between curcumin, resveratrol and IC chains. The idiosyncratic release kinetics between curcumin and resveratrol implies different molecular affinity between IC chains and these polyphenols, which can be influenced by the enclosed core material's size and polarity. The one stage release of IC:curcumin complexes indicates that the larger curcumin molecules are harder to come out from the IC network structure unless IC swells and dissolves in the presence of water. The two stage release nature of IC:resveratrol complexes points out that there are two mechanisms occurring simultaneously. The smaller size resveratrol molecules diffuse out easily from the IC water pockets with a concomitant IC network collapse. Thus, during the first stage, first-order diffusion is the main reason for the release and the collapse of IC matrix in the second stage.

The kinetics of final released amount (maximum loading) at different encapsulation times is shown in Fig. 4, which further offer the evidence about the affinity of curcumin and resveratrol to the IC chains. The linear fitting for the first three weeks and the later three weeks data yields the kinetic constant of the encapsulation efficiency. It is 3.44 for the resveratrol and 2.46 for curcumin for the first three weeks of encapsulation. The larger constant suggests faster nature of the polyphenol to complex with the IC network. Herein, with a higher value, resveratrol displays more affinity toward the IC network, which might be due to its smaller molecular size and also higher alcohol dissolution nature. Smaller size certainly aids molecule diffusion and penetration into the water pockets in the IC network, and the high dissolution ensures increased encapsulated concentration. The cross point of two fitted lines indicates the optimal encapsulation time for each polyphenol. The optimal encapsulation time of IC:curcumin is found to be 22 days, while that of IC:resveratrol is 21 days. This ideal encapsulation time could be useful for further experiments on other aspects of IC complexes.

4. Conclusions

In this study, crystalline and well-organized network structure of iota-carrageenan fibers has been used to encapsulate curcumin and

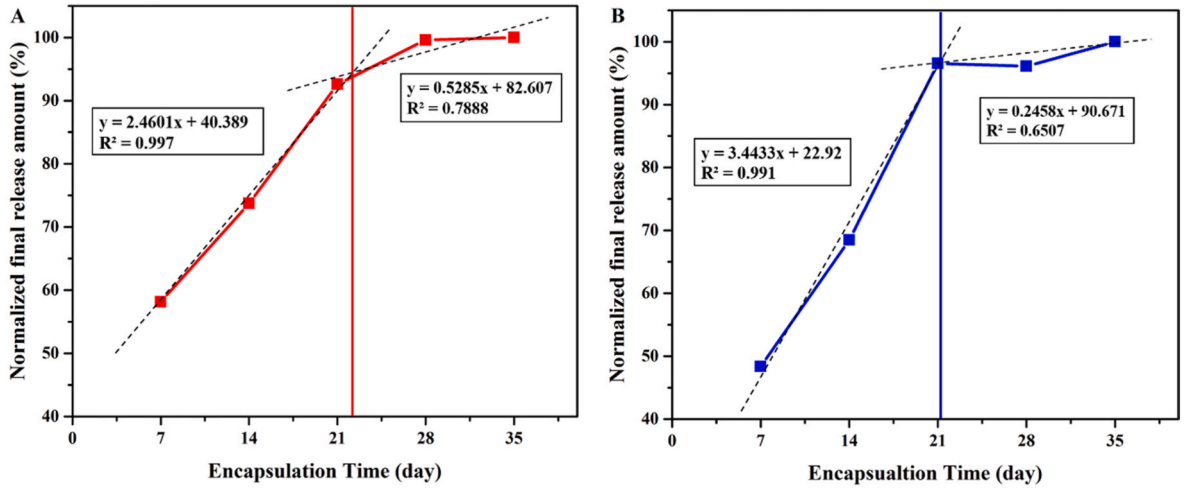

Fig. 4. The kinetics of release amount as a function of encapsulation time. (A) IC:curcumin and (B) IC:resveratrol.

resveratrol. The effect of encapsulation time has been studied. Structural characterization, thermal properties and the release kinetics of polyphenols from the IC:polyphenol complexes have been reported. The fiber X-ray diffraction data show the existence of ordered network structure in the complexes. The IC:curcumin complexes adopt an orthorhombic unit cell, while the IC:resveratrol complexes prefer the hexagonal net. These differences could be attributed to the size and affinity of curcumin and resveratrol molecules. The mDSC analysis provides the evidence for polyphenol protection by the IC network. The melting peaks of pure polyphenols are masked and the complexes possess higher exothermic and endothermic peaks than the pure IC fibers. The optimal encapsulation time of curcumin and resveratrol is found to be roughly 3 weeks. The release amount of resveratrol is two times higher than the curcumin suggesting that resveratrol is better suited to entrap in the iota-carrageenan network. The release kinetics of IC:curcumin could be explained based on the Korsmeyer-Peppas model. On the other hand, both first-order release and Korsmeyer-Peppas models are needed to understand the IC:resveratrol release nature.

There are a variety of polyphenol delivery systems such as modified starch, gums, porous starch, dextrin, liposomes, cyclodextrins, nanospheres, bacteria, protein coacervation and hydrocolloids. However, some of the lingering predicaments namely low water solubility, low stability and low bioavailability of polyphenols warrant alternatives. Our hydrocolloids-based carriers stand out tall due to their intrinsic low-cost, food grade, naturally safe and high bioaccessible nature. These new delivery systems could potentially provide cost-effective protection to polyphenols as well as any other molecule of interest against stresses such as heat, light, moisture and pH shift, to name a few. The application of such complexes could be envisioned to develop food supplements, functional foods and medicinal foods. However, further research is necessary to fully understand and take advantage of these delivery systems as the outcome could be extended to vitamins, flavors, drugs and even herbicides and pesticides, and forms our future direction.

CRediT authorship contribution statement

Tianming Yao: Investigation, Data curation, Formal analysis, Software, Visualization, Writing – original draft. **Srinivas Janaswamy:** Conceptualization, Methodology, Resources, Project administration, Funding acquisition, Supervision, Writing – review & editing.

Declaration of competing interest

Authors declare no conflict of interest.

Acknowledgements

Support is from the CSC (China Scholarship Council) program, Whistler Center for Carbohydrate Research and USDA National Institute for Food and Agriculture (SD00H648-18). We thank Dr. Irina Kosheleva and Dr. Robert Henning for help during the synchrotron X-ray intensity data collection. This research also used resources of the Advanced Photon Source, a U.S. Department of Energy (DOE) Office of Science User Facility operated for the DOE Office of Science by Argonne National Laboratory under Contract No. DE-AC02-06CH11357. Use of BioCARS was supported by the National Institute of General Medical Sciences of the National Institutes of Health under grant number P41 GM118217.

Appendix A. Supplementary data

Supplementary data to this article can be found online at https://doi.org/10.1016/j.foodhyd.2021.107466.

References

Aravind, S. M., Wichienchot, S., Tsao, R., Ramakrishnan, S., & Chakkaravarthi, S. (2021). Role of dietary polyphenols on gut microbiota, their metabolites and health benefits. *Food Research International*, Article 110189.

Avachat, A., & Kotwal, V. (2007). Design and evaluation of matrix-based controlled release tablets of diclofenac sodium and chondroitin sulphate. *Aaps Pharmscitech, 8*(4), 51–56.

Bermúdez-Soto, M.-J., Tomás-Barberán, F.-A., & García-Conesa, M.-T. (2007). Stability of polyphenols in chokeberry (Aronia melanocarpa) subjected to in vitro gastric and pancreatic digestion. *Food Chemistry, 102*(3), 865–874.

Canhada, S. L., Luft, V. C., Giatti, L., Duncan, B. B., Chor, D., Maria de Jesus, M., Matos, S. M. A., Molina, M., del, C. B., Barreto, S. M., & Levy, R. B. (2020). Ultra-processed foods, incident overweight and obesity, and longitudinal changes in weight and waist circumference: The Brazilian Longitudinal Study of Adult Health (ELSA-Brasil). *Public Health Nutrition, 23*(6), 1076–1086.

Castro-Barquero, S., Tresserra-Rimbau, A., Vitelli-Storelli, F., Doménech, M., Salas-Salvadó, J., Martín-Sánchez, V., Rubín-García, M., Buil-Cosiales, P., Corella, D., & Fitó, M. (2020). Dietary polyphenol intake is associated with HDL-cholesterol and a better profile of other components of the metabolic syndrome: A PREDIMED-plus sub-study. *Nutrients, 12*(3), 689.

Costa, P., & Lobo, J. M. S. (2001). Modeling and comparison of dissolution profiles. *European Journal of Pharmaceutical Sciences, 13*(2), 123–133.

Costa, P., & Sousa Lobo, J. M. (2003). Evaluation of mathematical models describing drug release from estradiol transdermal systems. *Drug Development and Industrial Pharmacy, 29*(1), 89–97.

Elfaruk, M. S., Wen, C., Chi, C., Li, X., & Janaswamy, S. (2021). Effect of salt addition on iota-carrageenan solution properties. *Food Hydrocolloids, 113*, Article 106491.

Fang, Z., & Bhandari, B. (2010). Encapsulation of polyphenols–a review. *Trends in Food Science & Technology, 21*(10), 510–523.

Feng, J.-Y., & Liu, Z.-Q. (2009). Phenolic and enolic hydroxyl groups in curcumin: Which plays the major role in scavenging radicals? *Journal of Agricultural and Food Chemistry, 57*(22), 11041–11046.

Gao, Z. (2011). Mathematical modeling of variables involved in dissolution testing. *Journal of Pharmaceutical Sciences, 100*(11), 4934–4942.

Gibaldi, M., & Feldman, S. (1967). Establishment of sink conditions in dissolution rate determinations. Theoretical considerations and application to nondisintegrating dosage forms. *Journal of Pharmaceutical Sciences, 56*(10), 1238–1242.
Gorzynik-Debicka, M., Przychodzen, P., Cappello, F., Kuban-Jankowska, A., Marino Gammazza, A., Knap, N., Wozniak, M., & Gorska-Ponikowska, M. (2018). Potential health benefits of olive oil and plant polyphenols. *International Journal of Molecular Sciences, 19*(3), 686.
Heikkilä, T., Salonen, J., Tuura, J., Hamdy, M. S., Mul, G., Kumar, N. al, Salmi, T., Murzin, D. Y., Laitinen, L., & Kaukonen, A. M. (2007). Mesoporous silica material TUD-1 as a drug delivery system. *International Journal of Pharmaceutics, 331*(1), 133–138.
Janaswamy, S., & Chandrasekaran, R. (2001). Three-dimensional structure of the sodium salt of iota-carrageenan. *Carbohydrate Research, 335*(3), 181–194.
Janaswamy, S., & Chandrasekaran, R. (2005). Cation-induced polymorphism in iota-carrageenan. *Carbohydrate Polymers, 60*(4), 499–505.
Janaswamy, S., & Chandrasekaran, R. (2006). Sodium ι-carrageenan: A paradigm of polymorphism and pseudopolymorphism. *Macromolecules, 39*(9), 3345–3349.
Janaswamy, S., Gill, K. L., Campanella, O. H., & Pinal, R. (2013). Organized polysaccharide fibers as stable drug carriers. *Carbohydrate Polymers, 94*(1), 209–215.
Janaswamy, S., & Youngren, S. R. (2012). Hydrocolloid-based nutraceutical delivery systems. *Food & Function, 3*(5), 503–507.
Korsmeyer, R. W., Gurny, R., Doelker, E., Buri, P., & Peppas, N. A. (1983). Mechanisms of solute release from porous hydrophilic polymers. *International Journal of Pharmaceutics, 15*(1), 25–35.
Korsmeyer, R. W., & Peppas, N. A. (1981). Effect of the morphology of hydrophilic polymeric matrices on the diffusion and release of water soluble drugs. *Journal of Membrane Science, 9*(3), 211–227.
Massounga Bora, A. F., Ma, S., Li, X., & Liu, L. (2018). Application of microencapsulation for the safe delivery of green tea polyphenols in food systems: Review and recent advances. *Food Research International, 105*, 241–249.
Ngwuluka, N. C., Ochekpe, N. A., & Aruoma, O. I. (2016). Functions of bioactive and intelligent natural polymers in the optimization of drug delivery. In *Industrial applications for intelligent polymers and coatings* (pp. 165–184). Springer.
Patras, A., Brunton, N. P., O'Donnell, C., & Tiwari, B. K. (2010). Effect of thermal processing on anthocyanin stability in foods; mechanisms and kinetics of degradation. *Trends in Food Science & Technology, 21*(1), 3–11.
Polowsky, P. J., & Janaswamy, S. (2015). Hydrocolloid-based nutraceutical delivery systems: Effect of counter-ions on the encapsulation and release. *Food Hydrocolloids, 43*, 658–663.
Prentice, A. M., & Jebb, S. A. (2003). Fast foods, energy density and obesity: A possible mechanistic link. *Obesity Reviews, 4*(4), 187–194.
Rajkumar, G., Al-Khayat, H. A., Eakins, F., Knupp, C., & Squire, J. M. (2007). The CCP13 FibreFix program suite: Semi-automated analysis of diffraction patterns from non-crystalline materials. *Journal of Applied Crystallography, 40*(1), 178–184.
Rasines-Perea, Z., & Teissedre, P.-L. (2017). Grape polyphenols' effects in human cardiovascular diseases and diabetes. *Molecules, 22*(1), 68.
Savoca, M., & Miller, C. (2001). Food selection and eating patterns: Themes found among people with type 2 diabetes mellitus. *Journal of Nutrition Education, 33*(4), 224–233.
Sriamornsak, P., Thirawong, N., & Korkerd, K. (2007). Swelling, erosion and release behavior of alginate-based matrix tablets. *European Journal of Pharmaceutics and Biopharmaceutics, 66*(3), 435–450.
Xing, Y., Lei, H., Wang, J., Wang, Y., Wang, J., & Xu, H. (2017). Effects of different drying methods on the total phenolic, rosmarinic acid and essential oil of purple perilla leaves. *Journal of Essential Oil Bearing Plants, 20*(6), 1594–1606.
Zhang, Y., Huo, M., Zhou, J., Zou, A., Li, W., Yao, C., & Xie, S. (2010). DDSolver: An add-in program for modeling and comparison of drug dissolution profiles. *The AAPS Journal, 12*(3), 263–271.